TRANSACTIONS OF THE INSTITUTE OF FLUID-FLOW MACHINERY

No. 137, 2017, 3–18

Katarzyna Jagodzińska*, Bartłomiej Hernik and Marek Pronobis

An analysis of coal and coal mine methane co-combustion in an 140 t/h pulverized coal boiler

Division of Boilers and Steam Generators, Institute of Power Engineering and Turbomachinery, Silesian University of Technology, Konarskiego 20, 44-100 Gliwice, Poland

Abstract

The paper presents an attempt to evaluate the impact of coal and coal mine methane co-combustion on the physics of the heat exchange in an 140 t/h pulverized-coal boiler through an analysis of 21 combinations of the boiler operating parameters – three different boiler loads (50, 75, and 100%) and seven values of the fired gas thermal contribution (0–60%). The obtained results are the temperature distribution of flue gas and steam in the boiler characteristic points, the heat transfer coefficient values for the boiler individual elements expressing the nature of changes in the heat transfer and the change in the boiler efficiency depending on how much gas is actually fired. An increase in the amount of co-fired gas involves a temperature increase along the flue gas path. This is the effect of the reduction in the amount of heat collected by the evaporator in the furnace. For these reason, the flue gas temperature at the furnace outlet rises by 9 K on average per a 0.1 increment in the fired gas thermal contribution. The temperature rise improves the heat transfer in the boiler heat exchangers – for the first- and the second-stage superheater the improvement totals 2.8% at a 10 pp. increase in the fired gas thermal contribution. However, the rise in the flue gas temperature at the boiler outlet involves a drop in the boiler efficiency (by 0.13 pp. for a rise in the fired gas thermal contribution by 0.1).

Keywords: Co-combustion; Methane; Heat transfer; Power boiler

*Corresponding Author. Email adress: katarzyna.jagodzinska@polsl.com

1 Introduction

Methane is a natural gas accumulated in hard coal beds. Both methane and hard coal were created at the same time – during decomposition of organic matter in the process of diagenesis (changes of vegetal matter into peat and lignite) and subsequent metamorphism (peat and lignite transformation into hard coal) [1,2]. The gas presents one of the greatest hazards directly related to hard coal mining. It forms an explosive mixture with air at the concentration of 5–15%. Therefore, its presence creates the risk of fire or coal dust explosion [3]. In order to prevent these risks, appropriate ventilation systems are used in the coal mine circulation paths. If the coal bed is characterized by a high content of CH_4, rock mass demethanization is also applied. The technologies of methane removal from coal beds are presented in [4,5].

It is estimated that about 60–70% of methane is released with ventilation air [6], in which methane concentration is maximum of 0.75% [7]; the rest is mine gas with a 30–70% content of CH_4. In the year 2007 about 268.8×10^6 m^3 of methane were captured from the total amount of methane in the area of hard cool mines of approximately 879.8×10^6 m^3 and about 165.7×10^6 m^3 were utilized, which is slightly over 60% of this number. The need of coal mining from beds located deeper and deeper causes growing trend of gas utilization. The main Polish tendency is to use mine gas as fuel for power boilers or other installations generating electricity and/or heat. Nevertheless, a considerable part of extracted methane is still fired in gas flares [3].

In the year 2007, methane emissions from hard coal mines constituted about 8% of the global anthropogenic emission of the gas, i.e., about 14% of total anthropogenic emissions of greenhouse gases worldwide [5,8]. Depending on the source, methane is characterized by the 21–23 times higher potential for causing the greenhouse effect than CO_2 [8,9]. Therefore, its utilization is not only financially profitable, but also important in terms of environmental protection, i.a., combustion of such gaseous fuel leads to reduction of particulate matter (PM) emission [10].

The coal beds with the highest content of methane in Poland are the ones grouped in the Jastrzębie Coal Company, and this is where the technology of mine gas utilization is being the most strongly developed. For example, the gas is co-fired with coal in an 140 t/h pulverized-coal (PC) boiler (OPG-140) in the 'Zofiówka' combined heat and power plant [11]. The analysis presented in this paper is based on this particular case. The boiler structure corresponds to that of a 140 t/h PC boiler fired with hard coal with the only exception of gas burners mounted on its side walls at the level of the first row of pulverized coal burners.

The boiler balance calculations are based on a 0-dimensional model using the methodology described in [12–14] and the data obtained from measurements. Measuring quantities are always burdened with a certain error. Therefore their use is limited in the model and the only ones assumed as error-free are the temperatures of the mediums at the boiler inlet and the pressures of the working mediums.

The furnace calculations are performed based on the (Central Boiler and Turbine Institution, CKTI, Russia) method adapted to the Polish conditions [12,13], whereas for the boiler convection part – calculations are made using the method presented in [14], based on many years of empirical research on Polish pulverized fuel boilers, which substantially improves the method accuracy compared to [12,13]. As a result, a fully balanced model is created in which the obtained mediums temperature distribution may be considered as reliable.

2 Input data

The thermal calculations are performed for the 140 t/h PC boiler presented in Fig. 1. The diagram includes markings of the boiler individual elements and temperatures of the mediums at their outlet and inlet. The markings correspond to those used during the calculations.

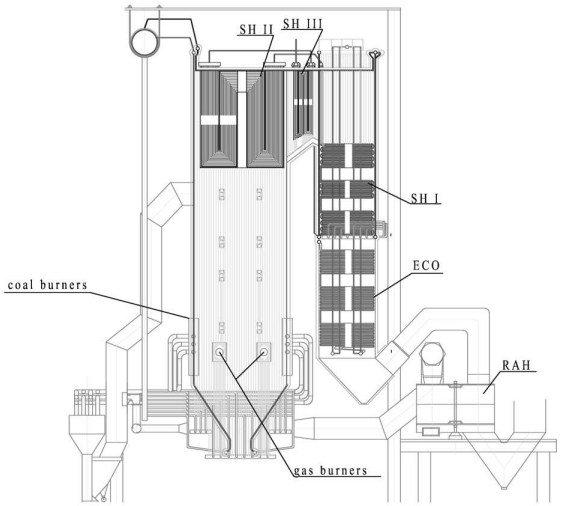

Figure 1: 140 t/h PC boiler diagram: SH I – 1st stage superheater, SH II – 2nd stage superheater, SH III – 3rd stage superheater, ECO – economizer, RAH – rotary air heater.

The boiler basic operating parameters and characteristic of combusted fuels used for the calculations are listed in Tabs. 1 and 2.

Table 1: Boiler operating parameters used for the calculations.

Quantity	Symbol	Value	Unit
Maximum continuous rating	$\dot{m}_s$	140	t/h
Live steam temperature	t_s	540	°C
Live steam pressure	p_s	9.8	MPa
Feed water temperature	t_{fw}	215	°C
Temperature of water in the attemperator	t_{w_att}	160	°C
Ambient temperature	t_{am}	20	°C
Carbon content in slag	C_s	7	%
Carbon content in fly ash	C_{fa}	5	%

Table 2: Characteristic of fired fuels in as received state (ar).

Quantity	Symbol	Value	Unit
Hard coal			
Lower heating value	LHV_c	21500	kJ/kg
Ash content	A^{ar}	23.5	%
Moisture content	M^{ar}	10.3	%
Carbon content	C^{ar}	54.2	%
Hydrogen content	H^{ar}	3.4	%
Sulphur content	S^{ar}	0.8	%
Oxygen content	O^{ar}	6.7	%
Nitrogen content	N^{ar}	1.1	%
Coal mine gas			
Lower heating value	LHV_g	18100	kJ/kg
Methane content	CH_4	50.89	$\%_{vol}$
Nitrogen content	N_2	40.39	$\%_{vol}$
Carbon dioxide content	CO_2	1.37	$\%_{vol}$
Oxygen content	O_2	7.35	$\%_{vol}$
Density in normal conditions	ρ_n	1.002	$kg/m^3{}_n$
Molecular mass	M_g	22.41	kg/kmol

3 Calculation results

This paper presents an analysis of changes in the boiler operating parameters resulting from changes in the load and in the amount of co-fired mine gas. The boiler nominal load (marked as 100%) and the outputs of 75 and 50% are taken into consideration. The changes in the co-fired gas amount are expressed by changes in the fuel thermal contribution, q_g, in the range from 0 (the reference case – coal fired only) to 0.6. Obtained temperature values in the boiler characteristic points are listed in Tabs. 3–5. They are corresponding to the boiler output values under analysis.

Table 3: Temperature distribution of media for the boiler load of 100%.

Parameter	Symbol	Unit	Value						
Gas thermal contribution	q_g	–	0	0.1	0.2	0.3	0.4	0.5	0.6
1	2	3	4	5	6	7	8	9	10
Flue gas temperature at the furnace outlet	t_{fg1}	°C	1098	1106	1109	1111	1115	1122	1129
Flue gas temperature at the 2nd stage superheater outlet	t_{fg2}	°C	806	812	813	813	816	820	824
Flue gas temperature at the 3rd stage superheater outlet	t_{fg3}	°C	711	715	715	715	717	719	721
Flue gas temperature at the 1st stage superheater outlet	t_{fg4}	°C	509	510	511	510	511	513	514
Flue gas temperature at the economizer outlet	t_{fg5}	°C	331	332	332	332	333	333	334
Flue gas temperature at the boiler outlet	t_{fg6}	°C	145	148	150	152	154	156	157
Feed water temperature	t_{fw}	°C	215	215	215	215	215	215	215
Water temperature downstream the economizer	t_{w2}	°C	278	280	280	280	281	282	282
Steam temperature at the 1st stage superheater inlet	t_{s2}	°C	310	310	310	310	310	310	310
Steam temperature at the 1st stage superheater outlet (pre-attemperation)	t_{s3}	°C	405	408	409	409	411	413	414
Steam temperature at the 2nd stage superheater inlet (post-attemperation)	t_{s3_att}	°C	357	353	353	351	350	349	350

Table 3: (continued).

1	2	3	4	5	6	7	8	9	10
Steam temperature at the 2nd stage superheater outlet (pre-attemperation)	t_{s4}	°C	486	483	485	482	481	482	484
Steam temperature at the 3rd stage superheater inlet	t_{s4_att}	°C	485	483	483	482	481	480	478
Steam temperature at the boiler outlet	t_{s5}	°C	540	540	540	540	540	540	540

Table 4: Temperature distribution of media for the boiler load of 75%.

Parameter	Symbol	Unit	Value						
Gas thermal contribution	q_g	–	0	0.1	0.2	0.3	0.4	0.5	0.6
1	2	3	4	5	6	7	8	9	10
Flue gas temperature at the furnace outlet	t_{fg1}	°C	993	998	1003	1008	1014	1028	1041
Flue gas temperature at the 2nd stage superheater outlet	t_{fg2}	°C	722	731	735	737	741	747	753
Flue gas temperature at the 3rd stage superheater outlet	t_{fg3}	°C	652	657	659	661	663	667	670
Flue gas temperature at the 1st stage superheater outlet	t_{fg4}	°C	472	474	475	475	476	478	480
Flue gas temperature at the economizer outlet	t_{fg5}	°C	310	312	314	314	314	316	316
Flue gas temperature at the boiler outlet	t_{fg6}	°C	127	129	132	134	136	139	141
Feed water temperature	t_{fw}	°C	215	215	215	215	215	215	215
Water temperature downstream the economizer	t_{w2}	°C	269	270	270	271	272	272	274
Steam temperature at the 1st stage superheater inlet	t_{s2}	°C	310	310	310	310	310	310	310
Steam temperature at the 1st stage superheater outlet (pre-attemperation)	t_{s3}	°C	385	387	389	390	392	394	396

Table 4: (continued).

1	2	3	4	5	6	7	8	9	10
Steam temperature at the 2nd stage superheater inlet (post-attemperation)	t_{s3_att}	°C	378	387	387	390	386	386	382
Steam temperature at the 2nd stage superheater outlet (pre-attemperation)	t_{s4}	°C	508	518	520	524	521	526	525
Steam temperature at the 3rd stage superheater inlet	t_{s4_att}	°C	502	499	498	497	496	494	492
Steam temperature at the boiler outlet	t_{s5}	°C	540	540	540	540	540	540	540

Table 5: Temperature distribution of media for the boiler load of 50%.

Parameter	Symbol	Unit	Value						
Gas thermal contribution	q_g	–	0	0.1	0.2	0.3	0.4	0.5	0.6
1	2	3	4	5	6	7	8	9	10
Flue gas temperature at the furnace outlet	t_{fg1}	°C	892	896	900	905	911	924	936
Flue gas temperature at the 2nd stage superheater outlet	t_{fg2}	°C	663	673	670	672	674	677	664
Flue gas temperature at the 3rd stage superheater outlet	t_{fg3}	°C	611	617	615	617	618	619	611
Flue gas temperature at the 1st stage superheater outlet	t_{fg4}	°C	457	460	459	459	460	460	457
Flue gas temperature at the economizer outlet	t_{fg5}	°C	310	311	311	311	311	313	313
Flue gas temperature at the boiler outlet	t_{fg6}	°C	154	156	157	159	160	162	163
Feed water temperature	t_{fw}	°C	215	215	215	215	215	215	215
Water temperature downstream the economizer	t_{w2}	°C	275	276	276	276	277	278	277
Steam temperature at the 1st stage superheater inlet	t_{s2}	°C	310	310	310	310	310	310	310
Steam temperature at the 1st stage superheater outlet (pre-attemperation)	t_{s3}	°C	389	391	391	392	393	395	393

Table 5: (continued).

1	2	3	4	5	6	7	8	9	10
Steam temperature at the 2nd stage superheater inlet (post-attemperation)	t_{s3_att}	°C	376	391	381	379	379	376	366
Steam temperature at the 2nd stage superheater outlet (pre-attemperation)	t_{s4}	°C	509	526	516	516	518	519	523
Steam temperature at the 3rd stage superheater inlet	t_{s4_att}	°C	509	505	506	505	505	503	507
Steam temperature at the boiler outlet	t_{s5}	°C	540	540	540	540	540	540	540

The boiler balance calculation values (losses, efficiency and fuel mass flow) and the most important parameters of the heat transfer in the boiler (values of the heat transfer coefficient on the flue gas side and of the heat exchanged in each boiler element) are gathered in Tabs. 6–10.

Table 6: Losses, efficiency and mass flows of fired fuels for the boiler load of 100%.

Parameter	Symbol	Unit	Value						
Gas thermal contribution	q_g	–	0	0.1	0.2	0.3	0.4	0.5	0.6
Stack loss	S_l	%	6.86	7.00	7.11	7.23	7.37	7.45	7.52
Boiler efficiency	η_b	%	91.39	91.25	91.14	91.02	90.89	90.81	90.73
Gas fuel mass flow	m_g	kg/s	0	0.62	1.23	1.85	2.46	2.78	3.09
Solid fuel mass flow	B_w	kg/s	5.16	4.65	4.14	3.62	3.12	2.86	2.60

Table 7: Losses, efficiency and mass flows of fired fuels for the boiler load of 75%.

Parameter	Symbol	Unit	Value						
Gas thermal contribution	q_g	–	0	0.1	0.2	0.3	0.4	0.5	0.6
Stack loss	S_l	%	5.84	5.94	6.13	6.25	6.38	6.53	6.66
Boiler efficiency	η_b	%	92.34	92.24	92.06	91.94	91.82	91.66	91.53
Gas fuel mass flow	m_g	kg/s	0	0.45	0.91	1.37	1.83	2.29	2.75
Solid fuel mass flow	B_w	kg/s	3.81	3.43	3.06	2.68	2.30	1.92	1.54

Table 8: Losses, efficiency and mass flows of fired fuels for the boiler load of 50%.

Parameter	Symbol	Unit	Value						
Gas thermal contribution	q_g	–	0	0.1	0.2	0.3	0.4	0.5	0.6
Stack loss	S_l	%	7.30	7.42	7.50	7.60	7.68	7.80	7.89
Boiler efficiency	η_b	%	90.75	90.63	90.55	90.45	90.37	90.25	90.17
Gas fuel mass flow	m_g	kg/s	0	0.31	0.62	0.92	1.23	1.55	1.86
Solid fuel mass flow	B_w	kg/s	2.59	2.33	2.07	1.82	1.56	1.30	1.05

Table 9: Heat transferred in the boiler individual elements for the load of 100, 75, and 50%.

Gas thermal contribution	q_g	–	0	0.1	0.2	0.3	0.4	0.5	0.6
Load		%	100						
2nd stage superheater	Q_{PEC_SHII}	MW	12.1	13.2	13.3	13.5	13.8	14	14.2
3nd stage superheater	Q_{PEC_SHIII}	MW	5.7	5.7	5.7	5.8	5.9	6	6.1
1st stage superheater	Q_{PEC_SHI}	MW	13	13	13	13	13.1	13.2	13.3
Economizer	Q_{PEC_ECO}	MW	10.9	10.9	10.9	10.9	11.0	11.1	11.1
Rotary air heater	Q_{PEC_RAH}	MW	9.7	9.6	9.6	9.5	9.5	9.5	9.4
Load		%	75						
2nd stage superheater	Q_{PEC_SHII}	MW	8.7	8.6	8.8	9	9.2	9.6	10.1
3rd stage superheater	Q_{PEC_SHIII}	MW	2.9	3.1	3.1	3.2	3.3	3.5	3.6
1st stage superheater	Q_{PEC_SHI}	MW	8.4	8.5	8.6	8.6	8.7	8.8	8.9
Economizer	Q_{PEC_ECO}	MW	7.1	7.3	7.4	7.4	7.4	7.5	7.5
Rotary air heater	Q_{PEC_RAH}	MW	7	6.9	7	6.9	6.9	6.9	6.8
Load		%	50						
2nd stage superheater	Q_{PEC_SHII}	MW	6	6	6.2	6.3	6.5	6.9	7.7
3rd stage superheater	Q_{PEC_SHIII}	MW	1.6	1.7	1.7	1.7	1.8	1.8	1.9
1st stage superheater	Q_{PEC_SHI}	MW	5.8	5.9	5.9	5.9	5.9	5.9	5.8
Economizer	Q_{PEC_ECO}	MW	5.3	5.4	5.4	5.4	5.4	5.4	5.4
Rotary air heater	Q_{PEC_RAH}	MW	4.9	4.9	4.8	4.8	4.8	4.7	4.7

It is assumed that changes in the amount of co-fired gas do not affect the state of ash deposits in the furnace and on the boiler individual heating surfaces, which remains the same.

Table 10: Flue gas-side heat transfer coefficient for the boiler load of 100, 75, and 50%.

Gas thermal contribution	q_g	–	0	0.1	0.2	0.3	0.4	0.5	0.6
Load		%	100						
2nd stage superheater	α_{fg_SHII}	W/m^{2}K	160.45	160.83	162.78	163.90	165.52	166.88	168.20
3rd stage superheater	α_{fg_SHIII}	W/m^{2}K	90.99	91.64	92.46	93.21	94.14	94.78	95.38
1st stage superheater	α_{fg_SHI}	W/m^{2}K	83.95	84.56	85.25	85.88	86.66	87.20	87.69
Economizer	α_{fg_ECO}	W/m^{2}K	119.08	119.89	120.66	121.36	122.18	122.72	123.20
Rotary air heater	α_{fg_RAH}	W/m^{2}K	121.79	122.56	123.19	123.80	124.51	124.96	125.38
Load		%	75						
2nd stage superheater	α_{fg_SHII}	W/m^{2}K	128.32	130.89	132.86	134.56	135.93	138.27	140.12
3rd stage superheater	α_{fg_SHIII}	W/m^{2}K	74.73	75.87	76.79	77.61	78.48	79.51	80.45
1st stage superheater	α_{fg_SHI}	W/m^{2}K	67.98	68.82	69.53	70.17	70.86	71.68	72.44
Economizer	α_{fg_ECO}	W/m^{2}K	98.04	98.88	99.65	100.29	100.97	101.84	102.58
Rotary air heater	α_{fg_RAH}	W/m^{2}K	99.83	100.50	101.31	101.81	102.36	103.17	103.73
Load		%	50						
2nd stage superheater	α_{fg_SHII}	W/m^{2}K	98.09	100.35	100.62	101.43	103.90	105.25	105.80
3rd stage superheater	α_{fg_SHIII}	W/m^{2}K	63.61	64.62	65.02	65.66	66.26	66.88	66.82
1st stage superheater	α_{fg_SHI}	W/m^{2}K	58.75	59.46	59.77	60.24	60.68	61.16	61.17
Economizer	αfg_ECO	W/m^{2}K	87.32	87.93	88.29	88.72	89.14	89.65	89.92
Rotary air heater	α_{fg_RAH}	W/m^{2}K	92.73	93.17	93.44	93.74	94.00	94.46	94.75

4 Analysis of obtained results

A rise in the thermal contribution of gas in the co-fired fuel mixture involves a rise in the flue gas temperature at the furnace outlet, T_{fgl}, (Tabs. 3–5). The increment is about 9 K on average for a rise in the gas thermal contribution, q_g, by 10 pp, which produces an increase in temperature by 45 K on average for q_g of 0.6. According to the semiempirical formula, which is the basis of the CKTI method, the temperature is expressed by the following relation:

$$T_{fgl} = T_c \frac{\mathrm{Bo}^{0.6}}{M a_f^{0.6} + \mathrm{Bo}^{0.6}}, \tag{1}$$

where: T_c – calorimetric combustion temperature, Bo – Boltzmann number, M – parameter taking into account the location of the maximum temperatures field, a_f – furnace equivalent emissivity.

Calorimetric combustion temperature, T_c, depends primarily on the co-fired fuel mixture calorific value and, therefore, it decreases by 3 K on average with a rise in the amount of fired gas q_g by 0.1. However, this change, has a smaller impact on the final value of temperature, T_{fgl}, compared to the effect of the Boltzmann number, Bo, and the furnace equivalent emissivity a_f. The Boltzmann number is mainly affected by the total mass flow of fired fuel. It is also inversely proportional to temperature T_c to the third power. The mass flow of the co-fired fuel mixture gets bigger as the amount of the gas increases. At the same time, temperature T_c decreases, which ultimately leads to a rise in Bo value that follows the increase in T_{fgl}. Moreover, a rise in the co-fired gas amount involves a decrease in the flame emissivity, a_{fl}, and, consequently, a drop in the furnace equivalent emissivity, a_f. This results from the gas combustion physics itself – a nonluminous flame is created during combustion of gas. It is characterized by worse radiative properties compared to the semiluminous flame arising during solid fuel combustion (due to the presence of fly ash and coke particles in flue gas). Therefore, the boiler evaporator absorbs less heat from flue gas and due to that the flue gas temperature at the furnace outlet is higher. The changes in the Boltzmann number, the flame emissivity and the furnace chamber equivalent emissivity are presented in Fig. 2.

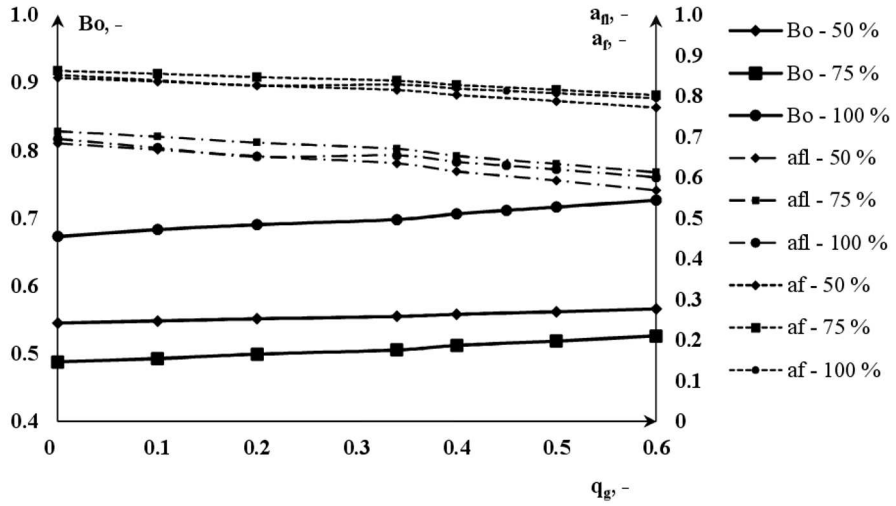

Figure 2: Boltzmann number, Bo, flame emissivity, a_{fl}, and the furnace equivalent emissivity, a_f, depending on the gas thermal contribution, q_g.

An increment in the flue gas temperature at the furnace outlet causes a rise in the flue gas temperature in each boiler element, which improves the heat transfer conditions in them. This is expressed by the values of the flue gas-side heat transfer coefficient, α_{fg}, (Tab. 10). The biggest change in α_{fg} can be observed in the case of the second and the third stage of steam superheater (Figs. 3 and 4), where the dominating heat transfer manner is radiation. Therefore these elements are chosen to present in this paper.

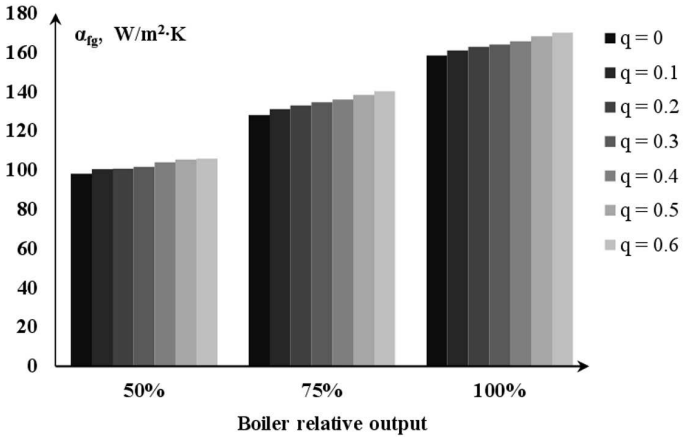

Figure 3: Heat transfer coefficient on the flue gas side in the 2nd stage of superheater.

Compared to the reference case, the increase in the co-fired gas thermal contribution to 0.6 involves a rise in the amount of transferred heat for the second and third stage of the superheater by 17% on average (Tab. 10, Figs. 5 and 6). Whereas for convective heat exchangers (first stage of superheater, economizer) the average rise totals 3%. The heat transfer intensification in convective exchangers results first and foremost from the increase in flue gas velocity. This is caused by increased amounts of flue gas in the case of a higher thermal contribution of the co-fired gas (the effect of the rise in the fired fuel mass flow). An exception is the regenerative rotary air heater, where the amount of transferred heat decreases with a rise in the co-fired gas amount, which results from the heat transfer coefficient on the air side. This is due to the smaller velocity of air in the exchanger resulting from the decrease in the mass flow of air needed for combustion (in the case of gas the theoretical demand for combustion air is smaller compared to hard coal).

A rise in temperature T_{fgl} involves also a rise in flue gas temperature at the boiler outlet (by 2 K on average per an increase in the gas thermal contribution

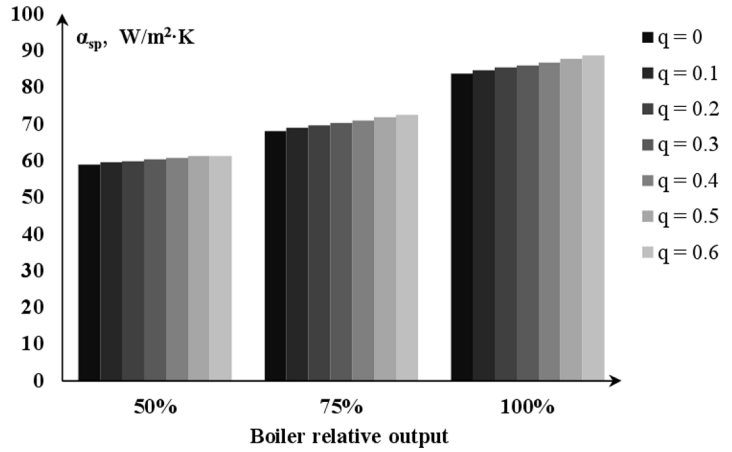

Figure 4: Heat transfer coefficient on the flue gas side in the 3rd stage of superheater.

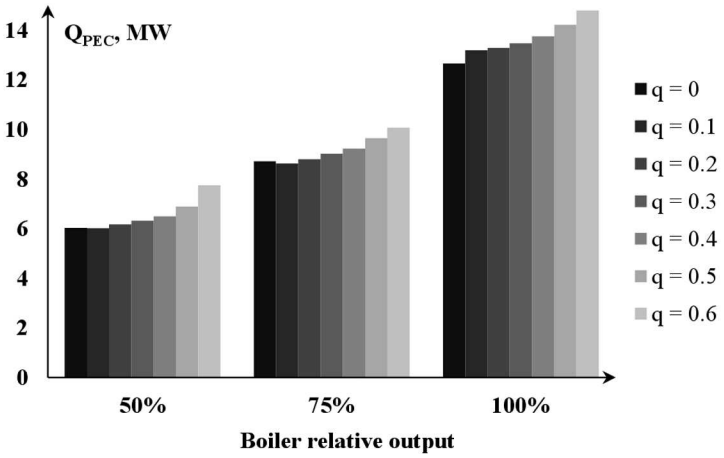

Figure 5: Heat transferred in the 2nd stage of superheater.

by 0.1), which causes a bigger stack loss (Tabs. 6–8). Consequently, if the contribution of co-fired gas is by 0.1 higher, the boiler efficiency, η_b, decreases by 0.12 and 0.15 pp. for the load of 50% and 75–100%, respectively.

The stack loss dependence on the gas thermal distribution is shown in Fig. 7; the drop in the boiler efficiency is illustrated in Fig. 8.

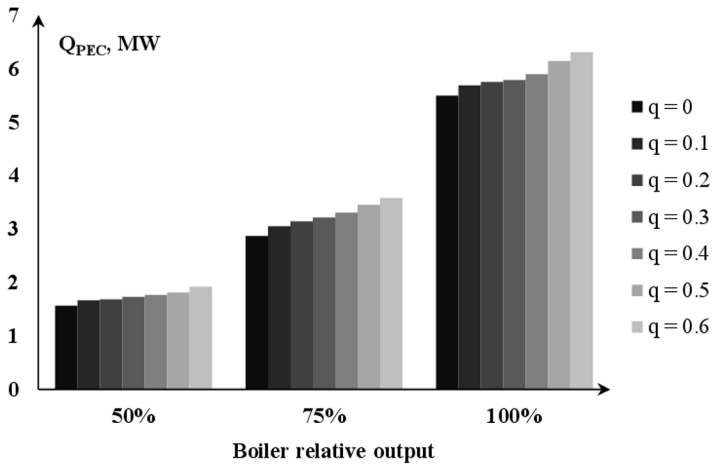

Figure 6: Heat transferred in the 3rd stage of superheater.

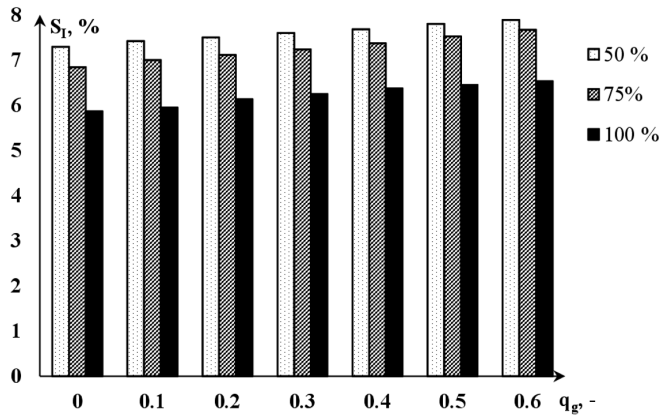

Figure 7: Stack loss depending on the gas thermal distribution for different boiler relative loads (50%, 75%, and 100%).

5 Summary and conclusions

The attempt to evaluate was undertaken the impact of mine gas co-combustion with hard coal in a 140 t/h PC boiler. The analysis is based on the boiler 0-dimensional model created according to the Russian computational method adapted to the Polish conditions. The calculations are performed for 21 cases

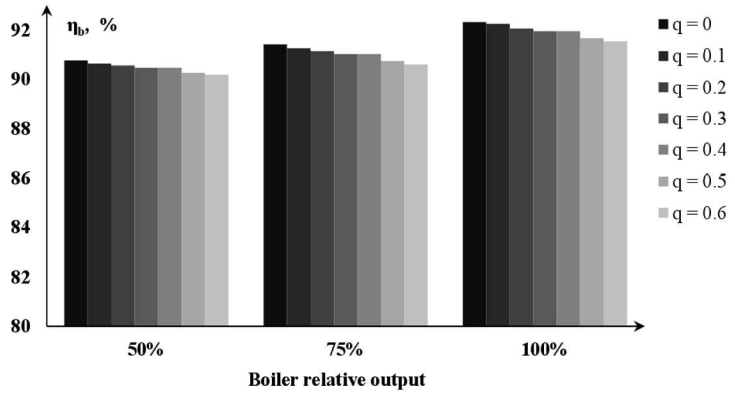

Figure 8: Drop in the boiler efficiency depending on the gas thermal distribution.

– for the boiler three relative loads (50, 75, and 100%) and for seven values of the co-fired gas thermal contribution included in the range from 0 to 60% (raised by 10% each time).

A rise in the co-fired gas amount involves a rise in the flue gas temperature values in individual points of the boiler. Compared to the reference case (hard coal combustion only), higher flue gas temperature at the furnace outlet causes a rise in the amount of heat transferred in the second and in the third stage of steam superheater by an average of 17% for $q_g = 0.6$. This results from the character of the heat transfer in these exchangers, where radiation, depending directly on the medium temperature raised to the fourth power, is the dominating manner.

The flue gas temperature at the boiler outlet rises as the amount of co-fired gas increases. This deteriorates the boiler efficiency due to the higher stack loss. The efficiency drop is about 0.13 pp on average per a 0.1 rise in the gas thermal contribution. This creates a need to fire just a slightly bigger amount of fuel compared to the fuel total amount.

Summing up, co-combustion of mine gas and hard coal affects the heat transfer in the boiler – the transfer gets intensified, first and foremost – in the second and in the third stage of superheater. However, this effect does not require any changes in the boiler design. This makes the solution attractive, both economically and ecologically, as a method of waste heat utilization without having to introduce costly modifications in existing boiler installations.

Received in November 2016

References

[1] Badyda K.: *Possibilities of mine gas utilization for power purposes in Poland*. Energetyka **648**(2008), 6, 416–423 (in Polish).

[2] Li G.: *Theoretical research and practice on coal mine methane extraction and ground development design*. Procedia Earth Planetary Sci. **1**(2009), 94–99.

[3] Karacan C. O., Ruiz F. A., Cote Michael, Phipps S.: *Coal mine methane: A review of capture and utilization practices with benefits to mining safety and to greenhouse gas reduction*. Int. J. Coal Geol. **86**(2011), 121–156.

[4] U.S. Environmental Protection Agency, *Coal Mine Methane Recovery: A Primer*. (2009).

[5] Su S., Beath A., Guo H., Mallett C.: *An assessment of mine methane mitigation and utilization technologies*. Prog. Energ. Combust. **31**(2005), 123–170.

[6] Gosiewski K., Pawlaczyk A., Jaschnik M.: *Combustion of coal-mine ventilation air methane in a thermal flow reversal reactor*. Przemysł Chemiczny (2011), 90/10, 1917–1923.

[7] Nawrat S., Napieraj S.: *An analysis of the possibility of utilization of ventilation air methane from the hard coal mine shafts in Poland*. Bezpieczeństwo Pracy i Ochrona Środowiska w Górnictwie (2010), 9, 22–29 (in Polish).

[8] Cheng Y., Wang L., Zhang X.: *Environmental impact of coal mine methane emissions and responding strategies in China*. Int. J. Greenh. Gas Con. **5**(2011), 157–166.

[9] Ostrowski P., Pronobis M., Remiorz L.: *Mine emissions reduction installations*. Appl. Thermal Eng. **84**(2015), 390–398.

[10] Dors M.: *Towards clean energy production*. Trans. Inst. Fluid-Flow Mach. **127**(2015), 91–116.

[11] Gatnar K.: *Economic utilization of coal bed methane on the example of the Jastrzębie Coal Company solutions*. In: Proc. 23rd Conf. 'Issues of energy resources and of energy in Polish economy', Zakopane, 11–14 Oct. 2009 (in Polish).

[12] Orłowski P., Dobrzański W., Szwarc E.: *Steam Boilers*. WNT, Warszawa 1979 (in Polish).

[13] Kuznetsov N.W., Nitor W.W., Dubovski I.E., Karasina E.S.: *Thermal Calculations of Steam Boilers. Standard Method*. Energia, Moscow 1973 (in Russian).

[14] Pronobis M.: *Heat exchange in the boiler convection surfaces with fouling*. Zeszyty Naukowe Politechniki Śląskiej, ser.: Energetyka, **115**, Gliwice 1992 (in Polish).